Submitted to *Physical Review B*, Sept. 2006.

Hydrogen-Helium Mixtures in the Interiors of Giant Planets

J. Vorberger,[1] I. Tamblyn,[2] B. Militzer,[1] and S.A. Bonev[2]

[1] *Geophysical Laboratory, Carnegie Institution of Washington, 5251 Broad Branch Road, NW, Washington, DC 20015*

[2] *Department of Physics and Atmospheric Science, Dalhousie University, Halifax, Nova Scotia B3H 3J5, Canada*

(Dated: September 28, 2006)

Equilibrium properties of hydrogen-helium mixtures under conditions similar to the interior of giant gas planets are studied by means of first principle density functional molecular dynamics simulations. We investigate the molecular and atomic fluid phase of hydrogen with and without the presence of helium for densities between $\rho = 0.19\ \mathrm{g\,cm^{-3}}$ and $\rho = 0.66\ \mathrm{g\,cm^{-3}}$ and temperatures from $T = 500\,\mathrm{K}$ to $T = 8000\,\mathrm{K}$. Helium has a crucial influence on the ionic and electronic structure of the liquid. Hydrogen molecule bonds are shortened as well as strengthened which leads to more stable hydrogen molecules compared to pure hydrogen for the same thermodynamic conditions. The *ab initio* treatment of the mixture enables us to investigate the validity of the widely used linear mixing approximation. We find deviations of up to 8% in energy and volume from linear mixing at constant pressure in the region of molecular dissociation.

I. INTRODUCTION

The discovery of the first extrasolar planet in 1995[1] marked the beginning of a new era in planetary science, which is characterized by great improvements in observational techniques and a rapidly expanding set of known extrasolar planets. Most of the about 200 known planets are giant gas planets in small orbits since the primary tool for detection, radio velocity measurement, is most sensitive for finding heavy planets that rapidly orbit their parent star[2,3]. From radius measurements of transient extrasolar planets, we know that most of the discovered planets consist primarily of hydrogen and helium. Therefore, there is a great need for accurate equation of state (EOS) data for these elements under giant gas planet conditions[4]. The knowledge of equilibrium properties of mixtures of hydrogen and helium will help to clarify questions concerning the inner structure, origin, and evolution of such astrophysical objects. Open questions are whether or not hydrogen and helium phase-separate inside giant planets, if a plasma phase transition[71] under the influence of helium can be found, and if a solid rocky core exists in Jupiter[4,5].

The EOS of hydrogen has attracted considerable attention and a large number of models have been introduced to characterize hydrogen at high pressure and temperature. Of great use in astrophysical calculations and planet modeling are (free energy) models operating in the chemical picture[6–13]. In these models, the hydrogen fluid is assumed to be composed of well-defined chemical species like atoms, molecules, and free charged particles. Such methods operate in the thermodynamic limit and are capable of describing large parameter regions of temperature and density. Further advantages of the free energy models are the small computational effort required to calculate the EOS and the explicit knowledge of all the considered contributions to the EOS. Ionization and dissociation degrees are computed by means of mass action laws and are not subject to fluctuations due to technical issues as in simulations. Atoms and molecules are treated as separate elementary species instead of being considered as bound states of electrons and nuclei. This implies certain approximations that limit the quality of these approaches. At sufficiently high density, the definition of atoms and molecules becomes imprecise as the lifetime of such objects decreases rapidly with density and mean distances between nuclei and electrons become comparable to bond lengths.

In this paper, special emphasis will be placed on testing the accuracy of the linear mixing approximation, which is often applied in free energy models to calculate the EOS of mixtures of different chemical species such as hydrogen and helium. A similar approach can be used to characterize mixtures of hydrogen atoms and molecules[8,14]. This approximation allows the calculation of thermodynamic variables of mixtures by a simple linear superposition of properties of pure substances. Linear mixing is a useful assumption to make if reliable experimental or theoretical data are only available for pure substances, or for cases where it has been shown that particles interact only weakly.

To avoid the shortcomings of chemical models, first principle calculations can be applied. Such methods work in the physical picture and treat electrons and nuclei as elementary particles interacting via the Coulomb potential. Quantum theory then describes the effects leading to the formation of atoms or molecules and their statistics. For hydrogen, there have been great efforts to study the equilibrium properties by means of density functional theory (DFT)[15–17], DFT-molecular dynamics (DFT-MD)[18–20], DFT - hypernetted chain equation combination (DFT-HNC)[21–23], path integral Monte Carlo (PIMC)[24,25], couple electron-ion Monte Carlo (QMC)[26], and Green's function theory[27,28].

Questions addressed include the problem of the hydrogen Hugoniot[29–32] and helium Hugoniot[33], the nature of

the transition in hydrogen from a molecular to an atomic state[24,34,35], the melting line of hydrogen[36], the different molecular solid phases[17,37–39], and the atomic solid (metallic Wigner crystal) proposed to be found at very high pressures[40–42]. Although DFT-MD is primarily an electronic groundstate method, it can be readily applied to describe dense solid and fluid hydrogen and helium at conditions relevant to giant gas planets because the electrons in such systems are either chemically bound or highly degenerate.

To our knowledge, there are only a few first principle calculations dealing with the question of the helium influence on the hydrogen EOS. Klepeis *et al.*[16] made predictions concerning the hydrogen-helium phase separation but the DFT method applied in that paper is not suitable to treat the high temperature liquid found inside giant gas planets since only lattices could be discussed. The first DFT-MD calculations, performed by Pfaffenzeller *et al.*[43], lead to more reasonable values for hydrogen-helium demixing. However, their simulations were performed using Car-Parinello MD (CP-MD). The high temperature region ($T \geq 15000$K) where partial ionization occurs was considered by Militzer[44].

Here we present new results concerning the hydrogen and hydrogen-helium EOS for conditions inside giant gas planets as derived from first principle DFT-MD. We use Born Oppenheimer MD (BO-MD) in order to ensure well converged electronic wavefunctions at every step. The density and temperature values chosen cover the region of molecular dissociation where we expect corrections to the linear mixing approximation to be most significant.

We continue with Section II which contains details of our computational method. Results for the hydrogen EOS are presented in Section III A and compared to EOS data from a variety of other approaches. Furthermore, the ionic and electronic structures of the hydrogen fluid and their dependence on temperature and density are investigated as well. The EOS and properties of hydrogen-helium mixtures are studied in Subsection III B. The focus there is on understanding how the presence of helium influences the stability of hydrogen molecules and the electronic structure, as well as on determining excess mixing quantities. Finally, the validity of the linear mixing approximation is examined in Subsection III C and Section IV provides a summary of our results and conclusions.

II. METHOD

We use first principle DFT-MD within the physical picture to describe hydrogen-helium mixtures under giant gas planet conditions. This means that protons as well as helium nuclei are treated classically. Nuclei and electrons interact via a Coulomb potential. Since $T \ll T_F$, where T_F is the Fermi-temperature, for all densities and temperatures found inside a typical giant gas planet, we employ ground state density functional theory to describe the electrons in the Coulomb field of the ions. The ions have sufficiently large mass to be treated as classical particles and their properties described well by means of molecular dynamics simulations. We employ the Born-Oppenheimer approximation to decouple the dynamics of electrons and ions. The electrons thus respond instantaneously to the ionic motion and the electronic wave functions are converged at every ionic time step. Compared to Car-Parinello MD, this reliably keeps the electrons in their ground state without the necessity to use an artificial electron thermostat for systems with a small band gap.

The calculations presented in this article were carried out with the CPMD package[45]. All MD results were obtained within the NVT ensemble. A Nosè-Hoover thermostat was applied to adjust the system temperature. The thermostat was tuned to the first vibration mode of the hydrogen molecule ($4400\,\mathrm{cm}^{-1}$). All DFT-MD simulations were with 128 electrons in super cells with periodic boundary conditions and convergence tests were performed with larger cells. An ionic time step of $\Delta t = 16$ a.u. (1 a.u. = 0.0242 fs) was used throughout, however we found that $\Delta t = 32$ a.u. is already sufficient for $r_s \geq 1.86$ in the hydrogen-helium mixtures. ($r_s = 3/\{(4\pi n)^{1/3} a_B\}$, r_s is the Wigner-Seitz radius, n the number density of electrons per unit volume). All simulations were run for at least 2 ps and for the calculation of thermodynamic averages, such as pressure and energy, an initial timespan of at least 0.1 ps was not considered to allow the system to equilibrate.

The DFT calculations were performed with plane waves up to a cutoff energy of $35 - 50$ Ha, the Perdew-Burke-Ernzerhof GGA approximation[46] for the exchange-correlation energy, and Γ-point sampling of the Brillouin zone. We used local Troullier-Martins norm conserving pseudopotentials[47,48]. The pseudopotentials were tested for transferability and for reproducing the bond length and groundstate energy of single hydrogen molecules as well as of helium dimers.

For each density, the simulations were started at low temperature where the system is in a molecular phase and the temperature was increased in steps of $\Delta T = 500$ K in order to avoid the premature destruction of molecules by temperature oscillations introduced by the thermostat.

The electronic density of states (DOS) were calculated for snapshots from MD simulations with the Abinit package[49] and using a Fermi-Dirac smearing. The presented results for DOS and bandgaps are based on multiple snapshots for each parameter set.

Finite size effects were tested for by carrying out simulations with supercells containing up to 324 electrons (plus the required neutralizing number of protons and helium nuclei). For densities corresponding to $1.86 \geq r_s \geq 1.6$ and at $T = 500$ K we found the changes in pressure and energy to be smaller than 2%. The convergence of the Brillouin zone sampling was checked by optimizing the electronic density of several MD snapshots with Γ-point, a 2×2×2, and a 4×4×4 Monkhorst-Pack grid of

k-points[50] for a $N_e = 128$ system. The Brillouin zone appears to be sufficiently small so that deviations between results with 1, 8, and 64 **k**-points are below 1% ($r_s = 1.6$, $T = 500\,\mathrm{K}$).

We also examined the significance of electronic excitations for the thermodynamic properties of the studied fluids. Snapshots from MD trajectories were taken and electronic states were populated according to a Fermi distribution corresponding to the MD temperature. For $r_s = 2.4$ and $T = 7000\,\mathrm{K}$ the pressure was found to increase by 8%. Since the degeneracy parameter of the electrons increases while moving along an isentrope to the center of a giant gas planet, this can be considered an upper limit for finite temperature electronic excitation effects; the error for higher densities and lower temperatures will be much smaller.

III. RESULTS

Here we present *ab initio* results for equilibrium properties of hydrogen and hydrogen-helium mixtures in a density region between $0.19\,\mathrm{g{\cdot}cm^{-3}}$ and $0.66\,\mathrm{g{\cdot}cm^{-3}}$ ($r_s = 2.4$ to $r_s = 1.6$) and for temperatures from 500 K to 8000 K. This parameter region includes part of the transition region from the molecular to the atomic fluid state of hydrogen and hydrogen-helium mixtures. It is, therefore, interesting to study not only to get insight into interior properties of giant gas planets but also to examine molecular dissociation, the molecular-atomic and the insulator-metal transitions in hydrogen. Additionally, one can consider the influence of helium on these transitions and properties of mixing.

A. Pure Hydrogen

Figure 1 provides a summary of our hydrogen EOS calculations using DFT-MD. Four different pressure isochores are shown. At low density ($r_s = 2.4$), the pressure increases monotonically with temperature as the character of the fluid changes smoothly from molecular to atomic. At this density, the transition is slow enough with temperature so that the drop in the pressure when molecules break (the interactions become less repulsive) is compensated by the increase of the kinetic contribution to the pressure.

At higher density ($r_s < 2$), the dissociation of molecules takes place more rapidly with increasing temperature and leads to a region of $\partial P/\partial T|_V < 0$. At sufficiently high density, this effect dominates over the pressure increase that results from the presence of two atoms instead of one molecule. Furthermore, the condition $\partial P/\partial T|_V < 0$ implies a negative thermal expansivity $\partial V/\partial T|_P < 0$, while the fluid maintains hydrostatic stability given by $\partial P/\partial V|_T > 0$.

By exhibiting a region with $\partial P/\partial T|_V < 0$, fluid hydrogen shares some properties with typical solids, where a

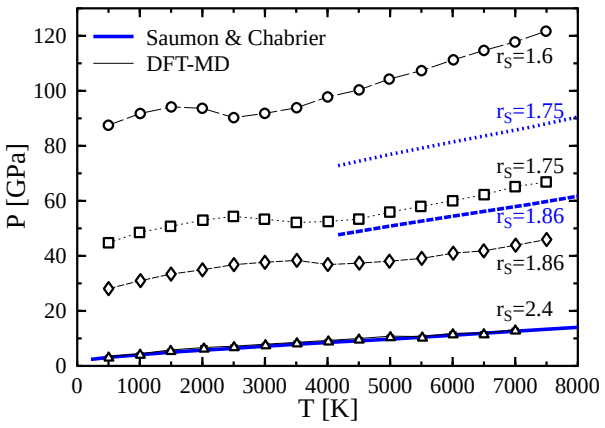

FIG. 1: Pressure-temperature relation for pure hydrogen along various isochores in DFT-MD (this work) and according to Saumon and Chabrier (SC)[7,8]. The isochore of SC for $r_s = 1.6$ lies out of the range of the P axis. Errors for the DFT-MD simulations are of the order of the symbols.

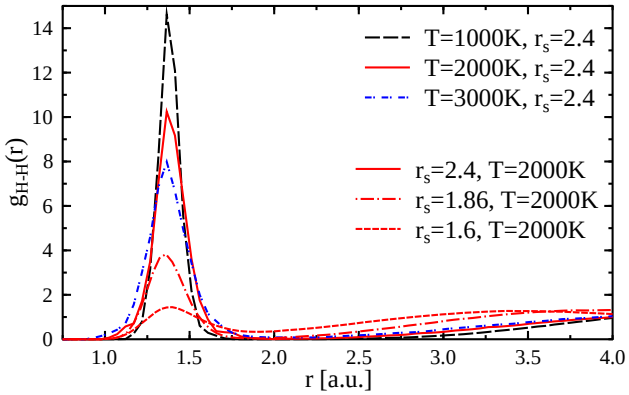

FIG. 2: Pair correlation functions $g(r)$ for pure hydrogen at different temperatures (color coded) and different densities: solid, dash-dotted, and dashed lines, respectively: $r_s = 1.6\,(0.66\,\mathrm{g\cdot cm^{-3}})$, $r_s = 1.86\,(0.42\,\mathrm{g\cdot cm^{-3}})$, $r_s = 2.4\,(0.20\,\mathrm{g\cdot cm^{-3}})$.

new crystal structure with more efficient packing appears and the pressure is lowered at fixed volume. In solid hydrogen different transition pressures to an atomic solid have been predicted, above 300 GPa[51,52] and $r_s =\sim 1.3$. This is consistent with the observed shift of the region of $\partial P/\partial T|_V < 0$ to lower temperatures, as the density is increased. It indicates a density effect on dissociation as less and less thermal energy is needed to break up the molecular bonds. At even higher densities than shown here, the bond length is equal or less than the mean particle distance. In this regime the interaction of molecules and atoms becomes too strong and pressure dissociation/ionization occurs.

Figure 2 shows the dependence of pair correlation functions (pure hydrogen at $r_s = 2.4$) on the temperature.

The first peak at $r \approx 1.40$ a.u. indicates the existence of hydrogen molecules With increasing temperature, the height of the first peak is reduced as molecules dissociate. An analogue behavior can be observed by plotting the changes in $g(r)$ with density. A strong decrease of the first peak with increasing density and thus a significant lower fraction of molecules at higher densities is revealed. In addition to the less pronounced first maximum, an overall weakening of the short range order can be observed with increasing temperature.

A more quantifiable picture of the described effects can be obtained by plotting the degree of dissociation,

$$\alpha = \frac{2N_{H_2}}{N_H} , \qquad (1)$$

as a function of temperature (Fig. 3). Here N_{H_2} is the average number of hydrogen molecules at the given density and temperature conditions. N_H the total number of hydrogen nuclei irrespectively of the dissociation state.

At higher density, fewer molecules are present at the same temperature as a result of pressure dissociation. While at low density, the dissociation proceeds gradually with temperature, the curves for $r_s \leq 1.75$ show a rapid drop around 2500 K, which is related to the $\partial P/\partial T|_V < 0$ region.

The dissociation degree and the binary distribution function are nevertheless not sufficient to draw a complete picture of the structure and dynamics in fluid hydrogen. The lifetime of the molecules must also be taken into account. Figure 3 shows that at $r_s = 1.75$, for example, even though on average more than 50% of the protons are found in paired states, the lifetime of these pairs is short (less than 2 H_2-vibrations on average); there is a continuous formation and destruction of pairs of hydrogen atoms. It is therefore imprecise to classify the fluid as either molecular-atomic or pure atomic as there is no unique criterion for a molecule. However, the results for the EOS obtained by our simulations do not depend on the number of molecules or atoms but only on temperature and density.

In addition to the dissociation of hydrogen molecules, of interest are the changes in the electronic structure taking place in the same parameter region. As the system becomes denser or the temperature is raised (still $T \ll T_F$), the interactions between the molecules in the fluid become stronger, and the formerly well-bound electrons become delocalized. This is associated with a strong increase in the electrical conductivity and is usually referred to as metallization[53]. The effect can be seen in the electronic density of states (DOS), namely the band gap, as shown in Fig. 4. We calculated the Kohn-Sham eigenvalues in GGA for several snapshots and estimated the bandgap in fluid hydrogen along the MD trajectory. For $r_s = 1.6$, a closing of the bandgap can be observed around $T = 2000K$. This means that a metallic-like state may have been formed. Furthermore, as indicated by the red lines in Fig. 4, the degree of dissociation incorporating lifetime effects decreases strongly

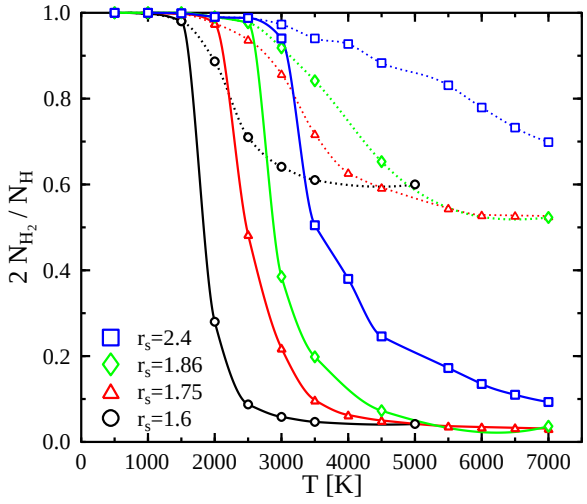

FIG. 3: Dissociation degree of the hydrogen molecules in pure hydrogen. The dissociation degree obtained by simply counting all pairs of hydrogen atoms with distance shorter than $r_{cut} = 1.8$ a.u. is plotted with dotted lines. Full lines take into account the lifetime of these pairs as well (10 H_2 vibrations at least to be counted as molecule).

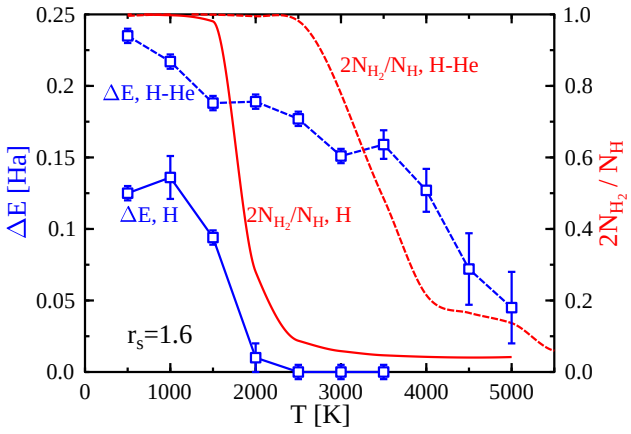

FIG. 4: Bandgap calculated in GGA for fluid hydrogen and hydrogen-helium mixture (blue curves) as well as dissociation degree for the two systems (red curves). The density corresponds to $r_s = 1.6$. The dissociation degree is determined by taking into account lifetime effects.

around the same temperature. To distinguish this degree of dissociation we do not consider proton pairs with less than 10 H_2 vibrations ($t = 10 \times 7.6$ fs) as being molecules. The closing of the bandgap and dissociation of hydrogen molecules happen at the same time.

It is well known that the GGA underestimates the bandgap. More sophisticated calculations[54] (for a H_2 solid) give a bandgap of ~ 0.6 Ha at $T = 300$ K. The value we obtain is 4 times smaller. Hood and Galli[55] compared values obtained with DFT (GGA) to quan-

tum Monte Carlo (QMC) gaps for liquid deuterium. For $T = 3000\,\mathrm{K}$ and $r_s = 1.6$, they found the QMC gap twice as large as the DFT gap. The actual temperature of metallization is thus somewhat higher. To improve the description of the electronic properties of the fluid, one needs to use a more accurate method than DFT-GGA, which is beyond the scope of this article. Still, it is worth noting that we find a continuous transition from an insulating to a conducting state, as determined by the closing of the gap. We do not observe molecules in the conducting phase as found by Weir *et al.*[53] or Johnson *et al.*[38].

While there is a general agreement about dissociation, ionic, and electronic structural changes throughout various papers, this agreement is only qualitative. As can be seen in Fig. 1, different methods give very different results for the EOS of dense fluid hydrogen. Whereas for the lowest density shown in Fig. 1, the agreement between the free energy model of Saumon and Chabrier[7,8] and our results is reasonable, deviations up to 20% (at $r_s = 1.86$) and even 24% (at $r_s = 1.75$ and above) can be found for higher densities. The free energy model overestimates the pressure considerably. The degrees of dissociation calculated with the free energy method show a significantly higher fraction of molecules than we find in our simulations. However, even a linear extrapolation of our pressure results of the molecular phase to higher temperatures (a linear scaling very similar to the one at $r_s = 2.4$ is assumed) only reduces the discrepancy with the result of Saumon and Chabrier but can not eliminate the difference completely. Deviations of this order may signify completely different physics inside giant gas planets and it is of great importance to discuss the discrepancies.

Comparisons with different first principle calculations can help resolve this issue, as agreement between different independent *ab initio* methods would be a strong indication for correct results. Figure 5 provides such a comparison. In addition to our results, PIMC data[29], wave packet molecular dynamic (WPMD) results[57,60,61] and older DFT-MD points[58] are shown. Furthermore, the isochores of two different models in the chemical picture are added: fluid variational theory (FVT)[56] as well as the linear mixing (LM) model[14]. They start from a mixture of atoms and molecules and their (Lennard-Jones type) interactions to minimize the free energy with respect to the fraction of the constituents. The isochore provided by WPMD deviates from the other ones by more than a factor of two at lower temperatures and by 25% at the highest temperatures shown here. PIMC is not a ground state method and is more capable of determining the EOS at higher temperatures. Information about fluid hydrogen or even about dissociation of hydrogen molecules can not be obtained. For higher temperatures, PIMC results lie between DFT-MD and FVT data. Better agreement is achieved between the two DFT-MD methods, FVT and LM. In the region with temperatures less than 10000 K some features of the curves are still different. The first

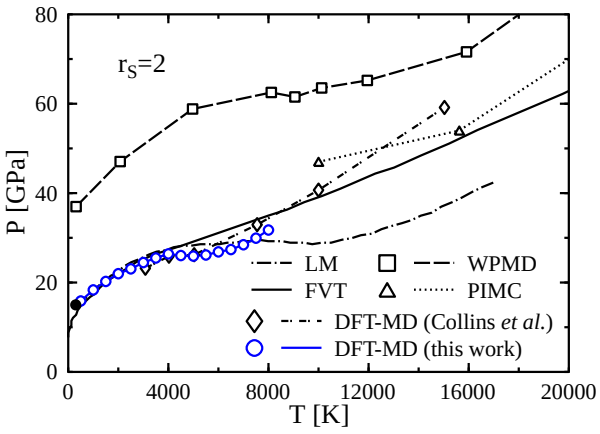

FIG. 5: Pressure-temperature relation for a single isochore of hydrogen with different methods for $r_s = 2$. Our DFT-MD results are shown in blue with circles. FVT by Juranek *et al.*[56] (solid black line), PIMC by Militzer *et al.*[29] (dotted line, triangles), WPMD by Knaup *et al.*[57] (dashed line, squares), DFT-MD by Collins *et al.*[58] (dashed, diamonds), LM by Ross[14] (long-short dashed), and this works DFT-MD results (blue, dots). The black dot indicates the pressure of a H_2-solid at $T = 300\,\mathrm{K}$[59]. The error bars of simulation results are within the size of the markers.

principle simulations show a region with a reduced or even slightly negative slope (smooth transition from a purely molecular to an atomic fluid) around 5000 K. Such a behavior is absent in the FVT model. The LM method, on the other hand, shows a similar feature but on a much wider temperature range. Thus, there is no unique picture of the EOS of dense fluid hydrogen. Deviations between the results of different first principle methods are related to the treatment of the electrons. Inconsistencies between the chemical picture, as a basis for FVT and LM, and the physical picture, as a foundation of DFT-MD or PIMC, contribute to the non-unique description. However that may be, DFT-MD provides reproducible results (the two DFT-MD studies were performed with different codes) and FVT seems to be reliable in the molecular fluid phase.

Lastly, we consider more closely the intermediate density range at a temperature typical for the interior of Jupiter. Figure 6 shows such an isotherm for $T = 5000\,\mathrm{K}$. Our result gives the lowest pressure. Saumon and Chabrier's EOS predicts a pressure up to 20% higher as stated above. The blue curve, as well as the green one, show a plasma phase transition (PPT). According to Saumon and Chabrier the PPT is expected at a density of approximately $\rho = 1\,\mathrm{g{\cdot}cm^{-3}}$ ($P = 200\,\mathrm{GPa}$). The FVT results with[13] or without[10] extension to ionized plasmas gives an isotherm right between the two above mentioned results. These methods predict a PPT at slightly smaller density of $\rho = 0.8\,\mathrm{g{\cdot}cm^{-3}}$ and $P = 100\,\mathrm{GPa}$). At both densities, neither we nor Weir *et al.*[53] have evidence for such a PPT. Instead, a continuous transition from a

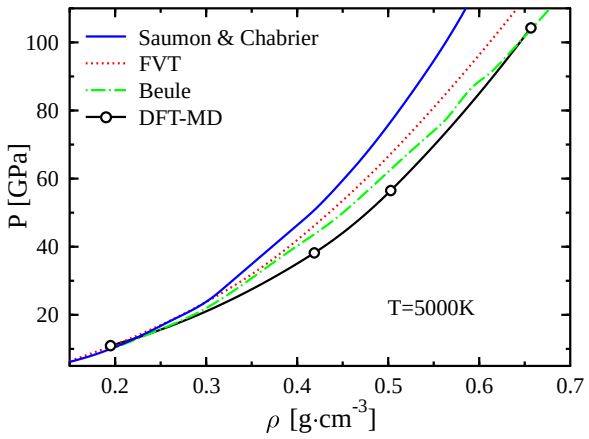

FIG. 6: The 5000 K pressure isotherm of hydrogen computed with various methods: this works DFT-MD (black with circles), FVT (red)[10], Beule (FVT+ionization, green)[13], Saumon and Chabrier (blue solid)[8]. HNC-MAL[12] gives similar results as FVT.

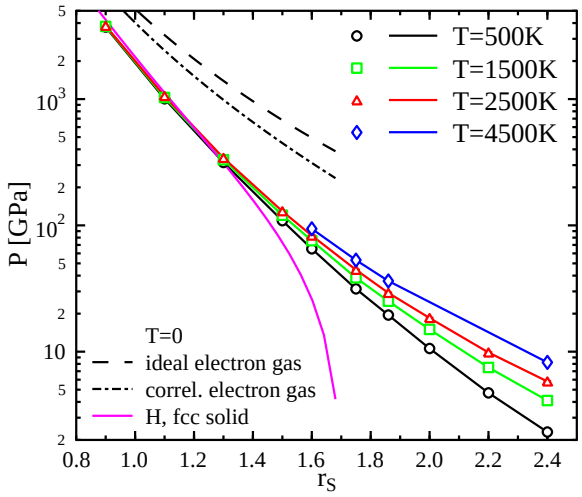

FIG. 7: Pressure isotherms of a mixture of hydrogen and helium (x=0.5) for different temperatures. High density limiting results for hydrogen and an electron gas are shown additionally.

molecular to an atomic state takes place at lower temperatures. It is nevertheless remarkable that the inclusion of ionization reduces the pressure and gives better agreement. From our simulation we have no information about possible intermediate ionized states of hydrogen.

B. Hydrogen-Helium Mixtures

So far we have studied pure hydrogen under giant gas planet conditions. A further degree of freedom is added if one considers a mixture of hydrogen and helium. Helium, even in small fractions, changes the EOS significantly. Helium has an influence on the formation and dissociation of hydrogen molecules, and it changes the ionic structure of the liquid as well as the electronic properties. The transition from a molecular state into an atomic state may be displaced or its character changed. Further, hydrogen and helium have been predicted to phase-separate in giant planet interiors.[6,62,63].

Models in the chemical picture use the linear mixing rule to add hydrogen and helium portions to the EOS[64]. Contributions from the entropy of mixing are ignored and all the interactions between the two subsystems are left out. First principle calculations include all these effects since a mixture of the two fluids can be simulated directly. The demixing line was calculated by classical Monte Carlo[65], by ground state DFT calculations[16], and by Car Parinello MD[43].

Here, we primarily present results for a hydrogen-helium mixture at a mixing ratio of $x = 0.5$. The mixing ratio is defined as

$$x = \frac{2N_{He}}{(2N_{He} + N_H)} , \qquad (2)$$

where N_H and N_{He} are the number of hydrogen and helium nuclei per unit volume. This definition weights the species according to the number of electrons that they contribute to the system. The corresponding Wigner-Seitz radius is computed from the total number of electrons. For many simulations, a mixing ratio of $x = 0.5$ was chosen so that large interaction effects between the two species could be observed.

Figure 7 shows the pressure for a number of isotherms for a hydrogen-helium mixture. The maximum density shown here corresponds approximately to conditions in the center of Jupiter ($r_s = 0.9$, $\rho = 3.6\,\mathrm{g\,cm^{-3}}$). It is demonstrated that temperature is not important for higher densities. since all the isotherms merge into the one with the lowest temperature. At the highest densities shown here the temperature contribution of the ions to the pressure is approximately 5%. The ions are strongly coupled and their interaction contribution to the EOS is of the order of 30%. The rest of the deviation from the ideal degenerate system is given by nonidealities in the electron gas and interactions between electrons and ions. For even higher densities the electronic contributions will become even more important since they rise with density as $n^{5/3}$ and thus faster than any other contribution.

The role of helium for the EOS of the mixture can be studied in Fig. 8. The pressure is slightly lowered over the whole temperature range, but more important is the fact that the region with negative $\partial P/\partial T|_V$ has vanished (for $x = 0.5$). The additional curve for Jupiter's hydrogen-helium mixing ratio (x=0.14) shows an intermediate step where the region with negative slope of the pressure does still exist but is reduced in markedness and in the temperature range of existence. More helium in the mixture means a shift of the negative slope to higher temperatures and a decrease of the depth of the minimum.

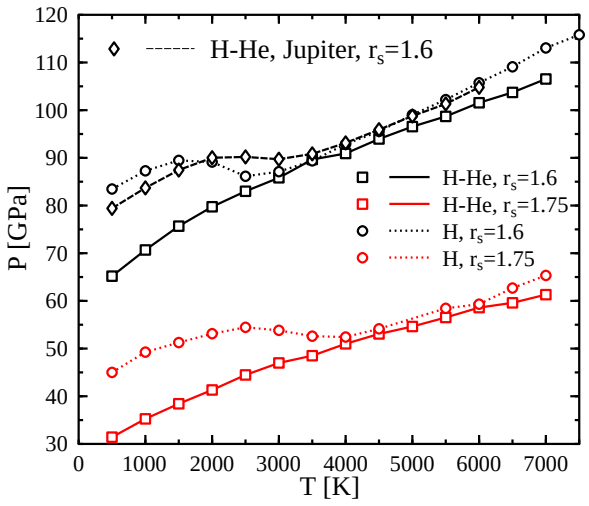

FIG. 8: Pressure isochores for a mixture of hydrogen and helium (x=0.5, solid lines) and for pure hydrogen (dotted lines) at two different densities. For $r_s = 1.6$ an additional curve for Jupiter's helium ratio (x=0.14) was added (back dashed line).

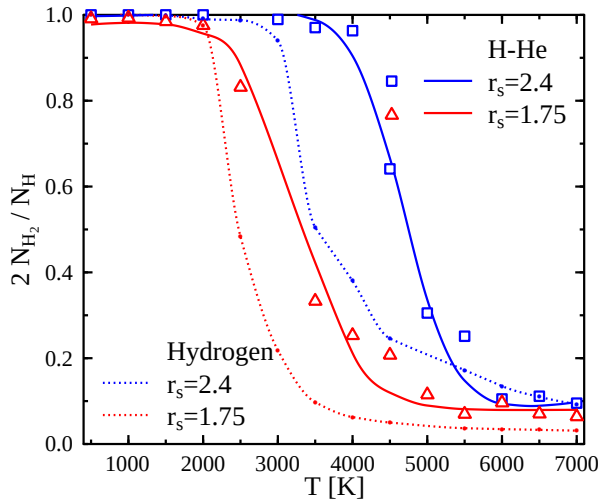

FIG. 9: Comparison of dissociation degrees (incorporating life time effects) in pure hydrogen and in hydrogen-helium (x=0.5). The solid lines are nonlinear fits to the data points.

For very high temperatures, the EOS of pure hydrogen and mixtures show a very similar behavior. Helium has a more significant influence on the pressure at lower temperatures.

These two different regions can clearly be assigned to different dissociation regimes (see Fig. 9). The transition from a molecular phase to an atomic phase, while still smooth, takes place at lower temperature and over a shorter range of temperature in hydrogen than in the mixture. This relatively rapid change in the microstructure of the fluid is the reason for the drop in the pressure. The vanishing of the molecules in hydrogen and their extended existence in the mixture can be confirmed with the help of pair correlation functions in Fig. 10. The molecular peak (first peak) drops considerably faster in pure hydrogen. This behavior and the higher peak in the mixture give clear evidence for molecules at the highest temperatures shown here. If we take the position of the first maximum as a measure for the mean bond length of the hydrogen molecule, we obtain a value of $\langle d \rangle = 1.37$ a$_0$ for pure hydrogen. In the mixture (with ratio of $x = 0.5$) this value changes to $\langle d \rangle = 1.29$ a$_0$ which means a shortening of the bond by 6%. The same can be obtained by means of nearest neighbor distributions as in Fig. 11. The first neighbor distribution considers the nearest neighbor only and effects of particles farther away are removed from the curve. Bond lengths obtained from Fig. 11 are slightly bigger. In addition, a shift of the bond length in hydrogen from 1000 K to 2000 K is revealed. The reduction of the bond length of 6% is confirmed. The latter value is in rather good agreement with data by Pfaffenzeller *et al.*[43]. The same conclusion is derived when comparing pair correlation functions for pure hydrogen and hydrogen-helium mixtures at constant pressure instead at constant electronic density.

Figure 9 describes the role of the (electronic) density during the process of dissociation. Helium stabilizes the molecules. This is due to the higher charge of $Z = 2$ of the helium nuclei. The intramolecular bonds depend strongly on the electronic behavior and the space available. If electronic wavefunctions between different molecules start to overlap, in other words, when Fermi statistic becomes important for the electrons of the system as a whole, and when the distances between the particles become so small that interactions between the molecules are no longer weak, the electrons are forced to delocalize to obey the Pauli exclusion principle and bonding becomes impossible. Helium under giant gas planet conditions, in atomic form, binds two electrons closely. The rest of the hydrogen atoms and electrons are affected less by density and temperature and the molecules remain stable over a wider range. The helium influence is thus two-part. First, its stronger Coulomb attraction binds electrons. Second, (as a consequence) it influences the many particle state of the electrons.

A phase diagram for molecular and atomic hydrogen and hydrogen-helium is provided in Fig. 12. Here, parameter regions for purely molecular, purely atomic as well as intermediate phases are shown. The diagram shows the increasing differences between hydrogen and the mixture with increasing pressure (density) and the huge differences (especially at high pressure) in the rate of the transition from a molecular to an atomic state. The transition region (from 95% to 5%) has nearly the same size for small pressures in pure hydrogen and in the mixture. At the other end of the pressure scale hydrogen changes from molecular to atomic over only 1500 K. In the mixture the changes are more moderate. At the pres-

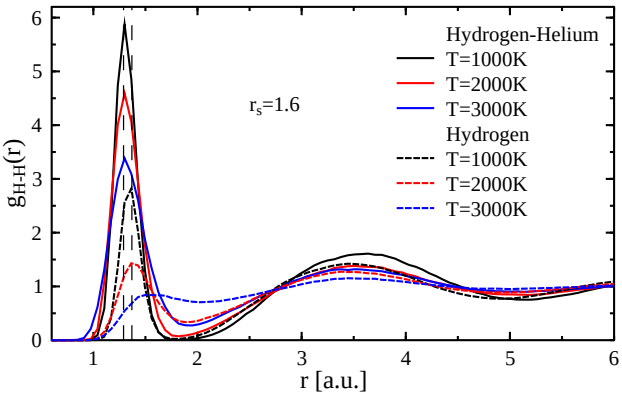

FIG. 10: Pair correlation functions for hydrogen (dashed lines) and hydrogen-helium (solid lines) at different temperatures. The order of the curves from top to bottom is the same as in the legend. The vertical thin dashed lines indicate the location of the first peak for hydrogen and hydrogen-helium, respectively.

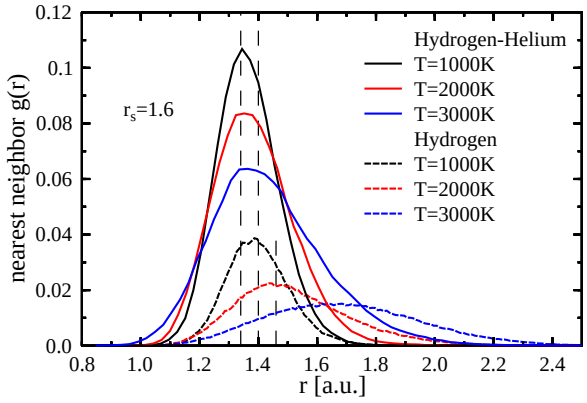

FIG. 11: 1st neighbor distribution for hydrogen (dashed lines) and hydrogen-helium (solid lines) at different temperatures. The order of the curves from top to bottom is the same as in the legend. The vertical thin dashed lines indicate the location of the peak for hydrogen and hydrogen-helium, respectively.

sures considered here, pressure dissociation is suppressed since the slope of the lines with constant dissociation degree is small for higher pressures. A good zeroth approximation for the behavior of the mixture is given by taking into account the hydrogen density only for the dissociation process. In this way, $r_s = 1.6$ for a 50% mixture of hydrogen and helium would correspond to $r_s = 2.02$ in pure hydrogen. This estimate works quite well for the 5% line, for instance.

Band structure and electronic density of states are affected also by helium. The inner regions of Jupiter are believed to be made of helium rich metallic hydrogen[4]. The conditions under which the mixture becomes metallic strongly depends on the amount of helium. A comparison of the (GGA) bandgaps in pure hydrogen and a

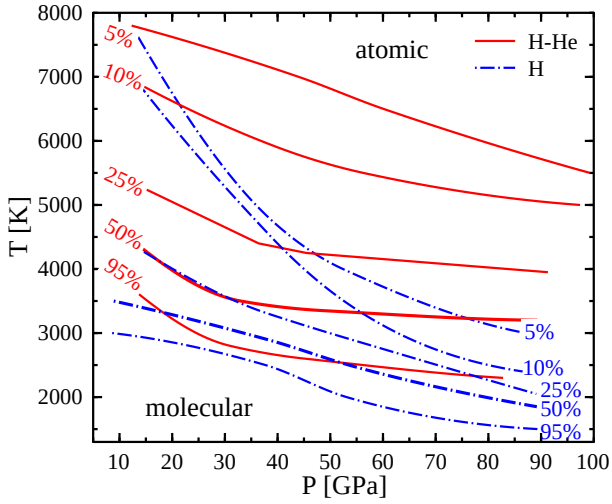

FIG. 12: Temperature-pressure-plane showing estimated lines of constant dissociation degree in pure hydrogen and in a hydrogen-helium mixture (x=0.5). The percentages give the fraction of hydrogen atoms bound in molecules.

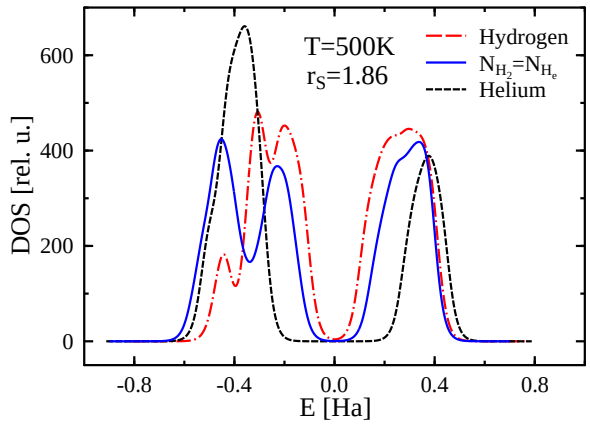

FIG. 13: Electronic density of states for pure fluid hydrogen, pure fluid helium, and for a mixture of hydrogen and helium (x=0.5) at fixed $T = 500\,\mathrm{K}$ and $r_s = 1.86$. The pressure is approximately 30 GPa. Curves shifted to agree at the Fermi energy (0 Ha) which is taken in the middle between HOMO and LUMO.

hydrogen-helium mixture ($x = 0.5$) is shown in Fig. 4. And while the bandgap in pure hydrogen goes to zero at relatively low temperatures, the gap in the mixture remains open over the whole temperature region shown. This can be traced back to the charge of the helium nucleus which shifts part of the Kohn-Sham eigenvalues to lower energies and thus increases the gap. The change in the electronic DOS from a helium system to a mixture to a pure hydrogen system is shown in Fig. 13. The black peak indicates atoms in fluid helium. The red curve shows mainly molecules in hydrogen and there are peaks resulting from intermolecular interaction, too. The blue

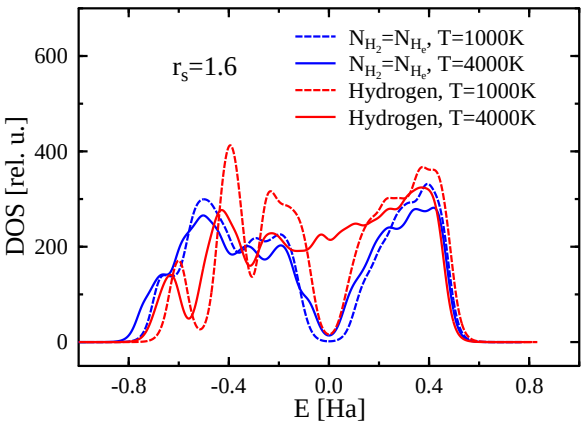

FIG. 14: Electronic density of states for pure fluid hydrogen and for a mixture of hydrogen and helium (x=0.5) as function of temperature. The pressure is approximately 100 GPa.

curve for the mixture is a superposition of the ones for pure systems, namely a helium peak to the left and a hydrogen molecule peak on the right hand side. The bands on the right hand side are empty since the curves are normalized so that the Fermi energy is at 0 Ha. The position of the edges of the bands at positive and negative energy strongly depends on the amount of helium in the fluid and therefore the width of the bandgap depends on the helium amount.

The dependence of the DOS on temperature is demonstrated in Fig. 14. We observe a similar effect as Scandolo did[34] although the transition from a mainly molecular liquid to an atomic fluid is smooth in our calculations. Due to the larger initial bandgap in the hydrogen-helium mixture and due to the effect of the helium described above, the bandgap for this systems remains, even at the highest temperature shown. Conversely, the gap in the pure system has completely closed at $T = 4000\,\mathrm{K}$.

C. Thermodynamic Properties of Mixtures

We will test the validity of a common approximation used in determining EOS's of mixtures. Most of the effort has been put into the determination of the EOS of pure systems. By ignoring the exact nature of the interaction between the pure phases, one can construct the EOS of any mixture of the original phases with the help of the linear mixing (LM) approximation

$$Y_{\mathrm{LM}} = (1-x)Y_{\mathrm{H}} + xY_{\mathrm{He}}\,, \tag{3}$$

with x according to Eq. (2) being the fraction of helium in the mixture and Y being a thermodynamic variable such as volume, pressure, or internal energy. For the free energy, an additional term describing the entropy of mixing must be included[14]. Linear mixing may be performed at constant chemical potential, at constant volume, or at constant pressure. For calculations of the internal structure of giant gas planets, mixing under constant pressure is the most important. In all cases, the deviation from LM can be calculated as

$$\Delta Y_{\mathrm{mix}}(x) = Y(x) - Y_{\mathrm{LM}}(x)\,, \tag{4}$$

where $Y(x)$ is the value obtained by DFT-MD for mixing fraction x and Y_{LM} is the LM value computed from independent simulations results for pure hydrogen and pure helium.

In this way it is assumed that the potential between particles of two different species can be written as an arithmetic average over the interactions in the pure systems[14]. This of course works for weak correlations only. The advantage is that one does not need to know exactly the interaction between, e.g., hydrogen and helium. This would be necessary for models in the chemical picture. Therefore, this approximation is used mainly by chemical models for the description of hydrogen-helium mixtures[7,8,13,56] or even mixtures of atoms and molecules of hydrogen[14]. The error introduced is difficult to quantify.

First principle calculations are able to verify the assumptions for LM and the validity of the approximation since these methods rely on the more fundamental Coulomb interaction, do not need to assume different interaction potentials between different species, and can thus simulate mixtures directly. There have been some investigations concerning the validity of LM by classical MC and integral equation techniques for classical binary liquids not including molecules[66–69]. In these cases, the deviations from LM found are of the order of 1% and below.

The first PIMC calculations for hydrogen-helium mixtures found deviations from LM at constant volume of up to 12% for temperatures between 15000 and 60000 K and giant gas planet densities ($r_s = 1.86$)[44]. This gives reason to expect that linear mixing might give a slightly falsified picture of the EOS of hydrogen-helium at lower temperatures, too. Again, since the conditions for phase separation depend strongly on small changes in the EOS (and thus from deviations from LM) it is crucial to investigate LM[70]. The advantage of first principle calculations is the correct treatment of the degenerate electrons and bound states, which is missing in the classical simulations.

The error introduced due to LM at constant volume (constant electronic density) as observed within DFT-MD is plotted in Fig. 15. Similar to the findings of other authors[44,69], the error is positive. As expected, the deviation in the pressure from the LM value is biggest for $x = 0.5$. Furthermore, increasing temperature causes an increase in the LM error of up to 12% for the highest temperature plotted in Fig. 15. The deviation from LM for a Jupiter like mixing ratio of $x \approx 0.14$ ranges from around zero ($T = 500\,\mathrm{K}$) up to 10%. The temperature inside Jupiter for this density is according to Saumon and Chabrier[7,8] of the order of 5000 K. This means that one

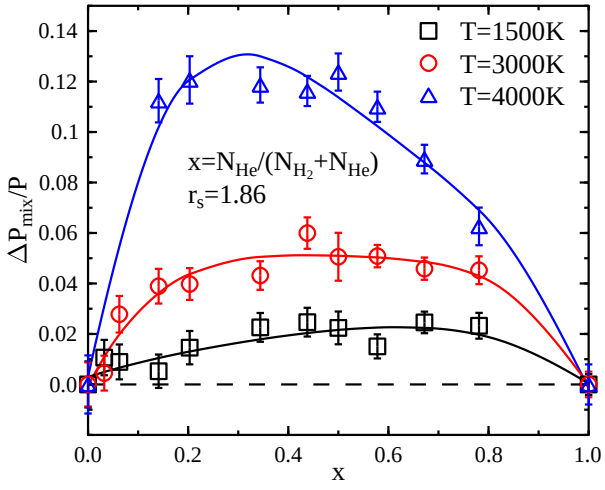

FIG. 15: Mixing error in the pressure due to the linear mixing approximation at constant volume for various temperatures as function of the mixing ratio. The electronic density is $r_s = 1.86$. This corresponds to $\varrho = 0.42\,\mathrm{g{\cdot}cm^{-3}}$ for pure H and $\varrho = 1.66\,\mathrm{g{\cdot}cm^{-3}}$ for pure He (pressure between 10 GPa and 40 GPa). The symbols represent calculated values, the lines were obtained with a polynomial fit of fourth order.

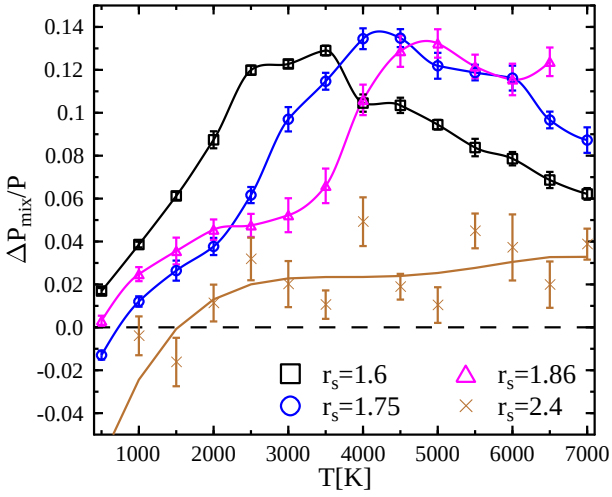

FIG. 16: Mixing error in the pressure due to the linear mixing approximation at constant volume for various densities as function of temperature. The mixing ratio is $x = 0.5$. The $r_s = 2.4$ data points suffer from simulation noise and the curve was obtained by least square fitting a third degree polynomial.

can expect a deviation of approximately 10% of the true EOS from the one calculated with LM.

The dependence of the error maximum at $x = 0.5$ from density and temperature is shown in Fig. 16. The curve for the smallest density shown here ($r_s = 2.4$) gives reason to conclude that LM is a good approximation for the

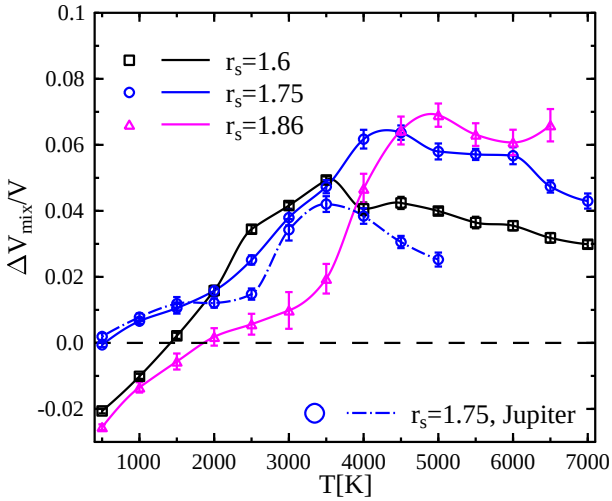

FIG. 17: Mixing error in the volume due to the linear mixing approximation at constant pressure for hydrogen-helium for various densities and two different mixing ratios of $x = 0.5$ (solid lines) and $x = 0.14$ (dashed line) as function of temperature.

pure molecular phase of hydrogen and helium as found at this density over a wide temperature range. With increasing density the deviations from LM start to grow as well and corrections to the pressure become significant for smaller temperatures. 5% error is reached around 3000 K for $r_s = 1.86$, around 2500 K for $r_s = 1.75$, and at approximately 1250 K for $r_s = 1.6$. The maximum of $\Delta P_{mix}/P$ is located at a slightly higher temperature than the transition from a pure molecular to a mainly atomic phase in pure hydrogen. The linear mixing rule transfers the behavior of pure hydrogen in an incorrect way into the mixture. This causes these deviations of up to approximately 15%. In addition, it is shown that linear mixing is not a good approximation for hydrogen-helium systems containing atoms *and* molecules. For higher temperatures the deviation from linear mixing declines although in the considered range it does not reach values below 5% again.

A similar statement can be made for mixing at constant pressure as shown in Fig.17. The same features as in Fig. 16 can be observed. The maximum of the mixing error is shifted to lower temperatures for higher densities. However, the error in the volume introduced by LM is slightly smaller than the one in the pressure. Comparing curves with different mixing ratios at constant density in Figs. 17 and 18 it is obvious that the maximum in the error is reached at lower temperatures for smaller mixing ratios x. This is in agreement with the temperature shift of molecular dissociation as function of the helium ratio in the system. Less obvious is the actual absolute value for the deviation from linear mixing. Whereas the error in the volume never exceeds 5%, the energy is much more sensitive to deviations from LM with an error of up to

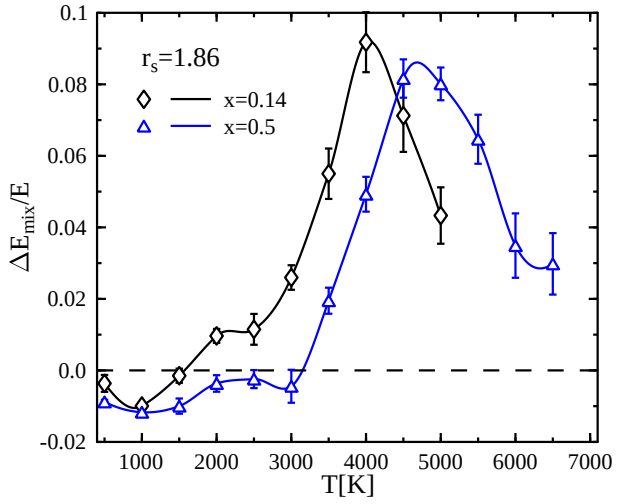

FIG. 18: Mixing error in the energy due to the linear mixing approximation at constant pressure as function of the temperature for hydrogen-helium mixtures at a density of $r_s = 1.86$. The mixing ratios are $x = 0.5$ and $x = 0.14$ (Jupiter).

9%.

All, figures 16, 17, and 18 show that LM can be considered a good approximation only for systems at low temperatures ($T < 1000K$) and at very high temperatures $T > 8000K$ for the densities presented here. In the case of liquid hydrogen-helium mixtures, these systems consist of weakly interacting hydrogen molecules and helium atoms (low T) or of weakly interacting hydrogen and helium atoms (high T). More complicated situations where atoms *and* molecules of hydrogen and helium are involved and interactions between them are non negligible require a better description than LM since helium has a significant influence on the dissociation degree and the mixture cannot be considered to be a composition of two fluids.

The figures presented here could suggest that LM is a rather good approximation for all of the higher temperatures. This is by no means the case. As stated before, LM works well only for nearly ideal systems. When the temperature becomes too high so that the gas of hydrogen and helium atoms experiences ionization (this can be accomplished by increasing the density as well) and a partially ionized plasma is created, the merely short ranged interatomic interactions are replaced by long range Coulomb forces and nonideality contributions to the EOS become very important again. In this regime, LM breaks down again, as was demonstrated by Militzer by means of PIMC[44].

IV. SUMMARY

We use first principle DFT-MD simulations to study equilibrium properties of hydrogen and hydrogen-helium mixtures under extreme conditions. The results obtained are relevant for the modeling of giant gas planets and for the principle understanding of the EOS of fluid hydrogen and hydrogen-helium mixtures.

Our results for pure hydrogen show a smooth transition from a molecular to an atomic state which is accompanied by a transition from an insulating to a metallic like state. In the transition region, we find a negative temperature derivative of the pressure. The results for the hydrogen EOS show deviations from widely used chemical models (up to 20%). In particular, the point of dissociation for the molecules is obtained at much lower temperatures than in chemical models. We find satisfying agreement with previous DFT-MD simulations only.

In particular, we demonstrate the influence of helium on hydrogen molecules. The presence of helium results into more stable molecules and an altered transition from a molecular to an atomic fluid state. Helium reduces the negative slope of the pressure isochores in the transition region. The bond length of the hydrogen molecules is shortened by 6% for $x = 0.5$. As a result, the degree of dissociation is lowered and the electronic bandgap is increased The effect of helium is found to be more important for higher densities where the stronger localization of the electrons prevents degeneracy effects for the electrons to become dominant.

Our analysis of the mixing properties for a $x = 0.5$ mixture of hydrogen and helium shows that the corrections to the linear mixing approximation are significant. Maximum EOS corrections of 15% were found for mixing at constant volume and 8% for mixing at constant pressure. For Jupiter like conditions, corrections up to 5% were obtained.

The presented results and forthcoming work should help to clarify long standing questions concerning the formation process of giant gas planets, help restrict the core size of Jupiter, and allow one to make predictions for the hydrogen-helium phase separation.

Acknowledgments

Fruitful discussions with B. Hubbard are acknowledged. This material is based upon work supported by NASA under the grant NNG05GH29G, by the Carnegie Institution of Canada, and by the NSF under the grant 0507321. I.T. and S.A.B. acknowledge support by the NSERC of Canada.

[1] M. Mayor and D. Queloz. *Nature*, 378:355, 1995.
[2] A. Burrows. *Nature*, 433:261, 2005.
[3] The extrasolar planet encyclopedia. http://exoplanet.eu.
[4] T. Guillot *el al.*, in *Jupiter*, F. Bagenal, Ed. (Univ. of Arizona Press, Tucson, 2003), chap. 3, pp. 35-57.
[5] D. Saumon and T. Guillot. *Astrophys. J.*, 609:1170, 2004.
[6] D.J. Stevenson. *Phys. Rev. B*, 12:3999, 1975.
[7] D. Saumon and G. Chabrier. *Phys. Rev. A*, 46:2084, 1992.
[8] D. Saumon, G. Chabrier, and H. M. Van Horn. *Astrophys. J. Suppl.*, 99:713, 1995.
[9] C. Winisdoerffer and G. Chabrier. *Phys. Rev. E*, 71:026402, 2005.
[10] H. Juranek, R. Redmer, and Y. Rosenfeld. *J. Chem. Phys.*, 117:1768, 2002.
[11] H. Juranek, V. Schwarz, and R. Redmer. *J. Phys A*, 36:6181, 2003.
[12] V. Bezkrovniy, M. Schlanges, D. Kremp, and W.-D. Kraeft. *Phys. Rev. E*, 69:061204, 2004.
[13] D. Beule, W. Ebeling, A. Förster, H. Juranek, S. Nagel, R. Redmer, and G. Röpke. *Phys. Rev. B*, 59:14177, 1999.
[14] M. Ross. *Phys. Rev. B*, 58:669, 1998.
[15] W. Kohn and L.J. Sham. *Phys. Rev.*, 140:A1133, 1965.
[16] J. E. Klepeis, K. J. Schafer, T. W. Barbee III, and M. Ross. *Science*, 254:986, 1991.
[17] I.I. Mazin and R. E. Cohen. *Phys. Rev. B*, 52:R8597, 1995.
[18] R. Car and M. Parrinello. *Phys., Rev. Lett.*, 55:2471, 1985.
[19] C. Winisdoerffer, G. Chabrier, and G. Zèrah. *Phys. Rev. E*, 70:026403, 2004.
[20] J. Kohanoff and J.-P. Hansen. *Phys. Rev. E*, 54:768, 1996.
[21] M. W. C. Dharma-wardana and F. Perrot. *Phys. Rev. B*, 66:014110, 2002.
[22] N.W.C. Dharma-wardana and F. Perrot. *Phys. Rev. A*, 26:2096, 1982.
[23] H. Xu and J.-P. Hansen. *Phys. Rev. E*, 57:211, 1998.
[24] W. R. Magro, D. M. Ceperley, C. Pierleoni, and B. Bernu. *Phys. Rev. Lett.*, 76:1240, 1996.
[25] C. Pierleoni, D.M. Ceperley, B. Bernu, and W.R. Magro. *Phys. Rev. Lett.*, 73:2145, 1994.
[26] C. Pierleoni, David M. Ceperley, and M. Holzmann. *Phys. Rev. Lett.*, 93:146402, 2004.
[27] M. Schlanges, M. Bonitz, and A. Tschttschjan. *Contr. Plasma Phys.*, 35:109, 1995.
[28] J. Vorberger, M. Schlanges, and W.-D. Kraeft. *Phys. Rev. E*, 69:046407, 2004.
[29] B. Militzer and D. M. Ceperley. *Phys. Rev. Lett.*, 85:1890, 2000.
[30] B. Militzer *et al. Phys. Rev. Lett.*, 87:275502, 2001.
[31] V. Bezkrovniy, V.S. Filinov, D. Kremp, M. Bonitz, M. Schlanges, W.-D. Kraeft, P.R. Levashov, and V.E. Fortov. *Phys. Rev. E*, 70:057401, 2004.
[32] S. A. Bonev, B. Militzer, and G. Galli. *Phys. Rev. B*, 69:014101, 2004.
[33] B. Militzer. *submitted to Phys. Rev. Lett.*, 2006.
[34] S. Scandolo. *Proc. Nat. Ac. Sci.*, 100:3051, 2003.
[35] O. Pfaffenzeller and D. Hohl. *J. Phys.: Condens. Matter*, 9:11023, 1997.
[36] S.A. Bonev, E. Schwegler, T. Ogitsu, and G. Galli. *Nature*, 431:669, 2004.
[37] V. Natoli, R.M. Martin, and D. Ceperley. *Phys, Rev, Lett.*, 74:1601, 1995.
[38] K.A. Johnson and N.W. Ashcroft. *Nature*, 403:632, 2000.
[39] H. Kitamura, S. Tsuneyuki, T. Ogitsu, and T. Miyake. *Nature*, , 2000.
[40] E. Wigner and H. B. Huntington. *J. Chem. Phys.*, 3:764, 1935.
[41] M.D. Jones and D.M. Ceperley. *Phys. Rev. Lett.*, 76:4572, 1996.
[42] B. Militzer and R. L. Graham. *Journal of Physics and Chemistry of Solids*, submitted (2005).
[43] O. Pfaffenzeller, D. Hohl, and P. Ballone. *Phys. Rev. Lett.*, 74:2599, 1995.
[44] B. Militzer. *J. Low. Temp. Phys*, 139:739, 2005.
[45] CPMD, Copyright IBM Corp 1990-2006, MPI für Festkörperforschung Stuttgart 1997-2001.
[46] J. P. Perdew, K. Burke, and M. Ernzerhof. *Phys. Rev. Lett.*, 77:3865, 1996.
[47] N. Troullier and J. L. Martin. *Phys. Rev. B*, 43:1993, 1001.
[48] M. Fuchs and M. Scheffler. *Comp. Phys. Com.*, 119:67, 1999.
[49] Copyright ABINIT group (M. Mikami, J. M. Beuken, X. Gonze) 2003-2005.
[50] H.J. Monkhorst and J.D. Pack. *Phys. Rev. B.*, 13:5188, 1976.
[51] P. Loubeyre, F. Occelli, and R. LeToullec. *Nature*, 416:613, 2002.
[52] D.M. Ceperley and B.J. Alder. *Phys. Rev. B*, 36:2092, 1987.
[53] S.T. Weir, A.C. Mitchell, and W.J. Nellis. *Phys. Rev. Lett.*, 76:1860, 1996.
[54] P. Giannozzi and S. Baroni. *Phys. Rev. B*, 30:7187, 1984.
[55] R. J. Hood and G. Galli. *J. Chem. Phys.*, 120:5691, 2004.
[56] H. Juranek and R. Redmer. *J. Chem. Phys.*, 112:3780, 2000.
[57] M. Knaup, P.-G. Reinhard, and C. Toepffer. *Contrib. Plasma Phys.*, 39 1-2:57, 1999.
[58] L. Collins, I Kwon, J. Kress, N. Troullier, and D. Lynch. *Phys. Rev. E*, 52:6202, 1995.
[59] P. Loubeyre, R. LeToullec, D. Hausermann, M. Hanfland, R.J. Hemley, H.K. Mao, and L.W. Finger. *Nature*, 383:702, 1996.
[60] M. Knaup. PhD thesis, University of Erlangen, Germany, 2002.
[61] M. Knaup, P.-G. Reinhardt, C. Toepffer, and G. Zwicknagel. *Comp. Phys. Com.*, 147:202, 2002.
[62] D.J. Stevenson and E.E. Salpeter. *Astrophys. J. Suppl. Ser.*, 35:221, 1977.
[63] D.J. Stevenson and E.E. Salpeter. *Astrophys. J. Suppl.*, 35:239, 1977.
[64] G. Chabrier, D. Saumon, W.B. Hubbard, and J.I. Lunine. *Astrophys. J.*, 391:817, 1992.
[65] W.B. Hubbard and H.E. deWitt. *Astrophys. J.*, 290:388, 1985.
[66] S. Ogata, H. Iyetomi, S. Ichimaru, and H.M. Van Horn. *Phys. Rev. E*, 48:1344, 1993.
[67] H.E. DeWitt, W. Slattery, and G. Chabrier. *physica B*, 228:21, 1996.
[68] Y. Rosenfeld. *Phys. Rev. E*, 54:2827, 1996.
[69] H.E. DeWitt and W. Slattery. *Contrib. Plasma Phys.*, 43:279, 2003.
[70] H.E. DeWitt. *Equation of State in Astrophysics*, page 330. IAU Colloquium 147. Cambridge University Press, 1994.
[71] phase transition connected with dissociation and ionization

of the neutral fluid